

Fast MAP Despeckling Based on Laplacian–Gaussian Modeling of Wavelet Coefficients

*Original*

Fast MAP Despeckling Based on Laplacian–Gaussian Modeling of Wavelet Coefficients / F., Argenti; Bianchi, Tiziano; A., Lapini; L., Alparone. - In: IEEE GEOSCIENCE AND REMOTE SENSING LETTERS. - ISSN 1545-598X. - 9:1(2012), pp. 13-17. [10.1109/LGRS.2011.2158798]

*Availability:*

This version is available at: 11583/2505887 since:

*Publisher:*

IEEE-INST ELECTRICAL ELECTRONICS ENGINEERS INC, 445 HOES LANE, PISCATAWAY, NJ 08855 USA

*Published*

DOI:10.1109/LGRS.2011.2158798

*Terms of use:*

This article is made available under terms and conditions as specified in the corresponding bibliographic description in the repository

*Publisher copyright*

(Article begins on next page)

# Fast MAP Despeckling Based on Laplacian-Gaussian Modeling of Wavelet Coefficients

Fabrizio Argenti, *Senior Member, IEEE*, Tiziano Bianchi, Alessandro Lapini, and Luciano Alparone

**Abstract**—The undecimated wavelet transform and the maximum a posteriori (MAP) criterion have been applied to the problem of SAR image despeckling. The MAP solution is based on the assumption that wavelet coefficients have a known distribution. In previous works, the generalized Gaussian (GG) function has been successfully employed. Furthermore, despeckling methods can be improved by using a classification of wavelet coefficients according to their texture energy. A major drawback of using the GG distribution is the high computational cost, since the MAP solution can be found only numerically. In this work, a new modeling of the statistics of wavelet coefficients is proposed. Observations of the estimated GG shape parameters relative to the reflectivity and to the speckle noise suggest that their distributions can be approximated as a Laplacian and a Gaussian function, respectively. Under these hypotheses, a closed form solution of the MAP estimation problem can be achieved. As for the GG case, classification of wavelet coefficients according to their texture content may be exploited also in the proposed method. Experimental results show that the fast MAP estimator based on the Laplacian-Gaussian assumption and on classification of coefficients reaches almost the same performances as the GG version in terms of speckle removal, with a gain in computational cost of about one order of magnitude.

**Index Terms**—Despeckling, synthetic aperture radar (SAR) images, undecimated wavelet transform (UDWT), maximum a-posteriori probability (MAP) estimation.

## I. INTRODUCTION

**S**PECKLE removal is a major concern in the analysis of synthetic aperture radar (SAR) images. Speckle noise is a granular disturbance that affects the observed reflectivity. Usually, it is modeled as a multiplicative noise: this nonlinear behavior makes the process of original information retrieval a nontrivial task [1]. In recent years, multiresolution analysis tools have been successfully applied to despeckling [2]–[5]. Several solutions were proposed based on the maximum a-posteriori probability (MAP) criterium and different distributions: the  $\Gamma$ -distribution [4], the  $\alpha$ -stable distribution [2], the Pearson system of distributions [3], the generalized Gaussian (GG) [6] [7], just to mention some examples.

In [6], it has been shown that the MAP criterion in the undecimated wavelet domain, associated with the GG distribution, leads to the following procedure: 1) estimation of

the spatially varying parameters of the GG distribution of the wavelet coefficients associated to the speckle-free reflectivity and to the speckle noise; 2) solution of the MAP equation. The method in [6] has been refined in [7], where a model to classify wavelet coefficients according to their texture energy was introduced. Wavelet coefficients are partitioned into classes having different degrees of heterogeneity, so that different GG parameters can be used for different sets of coefficients. The experimental results in [7] demonstrated that the proposed filtering approach outperformed previously proposed filters.

One of the major drawbacks of GG-based MAP solutions, either with or without classification of wavelet coefficients, is that they can be achieved only numerically, thereby leading to a high computational cost. In this letter, we propose a fast MAP despeckling based on an alternative modeling of wavelet coefficients. Experimental results suggest that the estimated distributions of the wavelet coefficients relative to the speckle-free reflectivity and to the speckle noise approximately follow a Laplacian and a Gaussian distribution, respectively. Under these assumptions, it is shown that the MAP equation can be solved in a closed form. Even if the Laplacian-Gaussian (LG) assumption has been already used to derive MAP and MMSE estimators [8], previous approaches were based on homomorphic filtering, which may induce a biased estimation. To the best of our knowledge, a clear assessment of the merits of the LG model in the case of non-homomorphic filtering of SAR images is not available in the literature.

As in the case of the GG-based MAP solution, also for the LG based method an improvement in performances can be achieved by using a classification of wavelet coefficients according to their texture content. The main idea is that segmentation can be used, at a very little additional cost, to select classes of wavelet coefficients to which apply different fast filters, or even no filtering at all. The computational cost can be reduced of one order of magnitude or more with respect to the solution obtained numerically with the GG assumption, without significantly affecting the performance in terms of speckle reduction.

This letter is organized as follows. In Section II, the MAP solution for despeckling SAR images is reviewed and the observations at the basis of the new proposed LG modeling of wavelet coefficients are described. In Section III, the closed form solution relative to the LG model is proposed; a refined version of the filter, based on the segmentation of wavelet coefficients, is illustrated as well. In Section IV, the experimental results, carried out both on synthetically degraded images and on real SAR acquisitions are presented. In Section V, some conclusions are drawn.

Copyright (c) 2011 IEEE. Personal use of this material is permitted. However, permission to use this material for any other purposes must be obtained from the IEEE by sending a request to pubs-permissions@ieee.org.

Manuscript received on Month Day, Year. This study has been carried out under the financial support of Italian Space Agency (ASI), COSMO-SkyMed Scientific Projects, under contract I/043/09/0.

The authors are with the Dipartimento di Elettronica e Telecomunicazioni, University of Florence, Via di Santa Marta, 3 - 50139 - Firenze - Italy, E-mail: {fabrizio.argenti,tiziano.bianchi,alessandro.lapini}@unifi.it, alparone@lci.det.unifi.it

## II. MAP DESPECKLING IN THE UNDECIMATED WAVELET DOMAIN

In this section, some results from [6] are reviewed and the experimental observations that lead us to a new wavelet coefficients modeling are presented.

### A. Signal model and undecimated wavelet transform

It is assumed that the observed signal follows the model

$$g[n] = f[n] \cdot u[n] = f[n] + f[n] \cdot (u[n] - 1) = f[n] + v[n], \quad (1)$$

where  $g[n]$  is the observed signal;  $f[n]$  is the speckle-free reflectivity we would like to estimate;  $u[n]$  is the speckle noise;  $v[n]$  accounts for speckle disturbance in the equivalent additive model. The speckle  $u[n]$  is assumed as white and independent from  $f[n]$ , whereas  $v[n]$  is signal-dependent. For the simplicity's sake, the model is formulated in one dimension.

Let  $W_x^{[j]}$  be the undecimated wavelet operator applied to the signal  $x$ . It performs a multiresolution decomposition, where  $j$  is the level of the decomposition. Thanks to the linearity of the operator, we have

$$W_g^{[j]}[n] = W_f^{[j]}[n] + W_v^{[j]}[n]. \quad (2)$$

To simplify the notation, the level  $j$  and the index  $n$  (when not strictly necessary) are omitted in the following.

Despeckling in the multiresolution domain means estimating the speckle-free wavelet coefficients  $\hat{W}_f[n]$  and applying the inverse undecimated wavelet transform.

### B. MAP estimation

The MAP estimator of the speckle-free wavelet coefficients is given by

$$\hat{W}_f = \arg \max_{W_f} p(W_f | W_g), \quad (3)$$

or, after applying the Bayes rule and the log function, by the equation

$$\hat{W}_f = \arg \max_{W_f} [\log p(W_g | W_f) + \log p(W_f)] \quad (4)$$

### C. Analysis of the GG Shape Parameter

In [6], a GG function is proposed to model the wavelet coefficients pdf's involved in (4). The zero-mean GG distribution is given by

$$p_{GG}(\theta) = \frac{\nu \eta}{2\Gamma(1/\nu)} e^{-(\eta|\theta|)^\nu}, \quad (5)$$

where  $\eta = \sigma^{-1}[\Gamma(3/\nu)/\Gamma(1/\nu)]^{1/2}$  is a *scale* parameter and  $\nu$  is a *shape* parameter. It is well-known that the GG distribution coincides with the Laplacian distribution for  $\nu = 1$  and with the Gaussian distribution for  $\nu = 2$ . In [6], it is shown that the shape parameter can be estimated by solving the following equation

$$\frac{E[X^2]}{\sqrt{E[X^4]}} = \frac{\Gamma(3/\nu)}{\sqrt{\Gamma(1/\nu)\Gamma(5/\nu)}}, \quad (6)$$

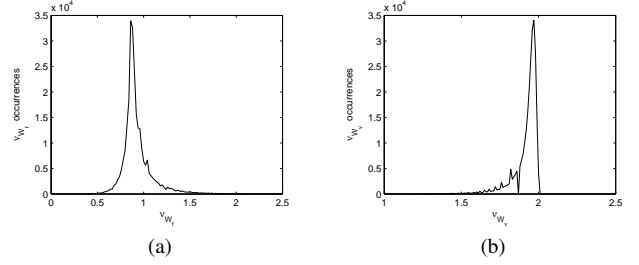


Fig. 1. Examples of the histogram of the estimated shape parameters: (a) wavelet coefficients of the speckle-free signal; (b) wavelet coefficients of the signal-dependent noise.

where  $E[X^2]$  and  $E[X^4]$  are the second and the fourth-order moments of the GG-distributed random variable  $X$ . In the actual implementation, such moments are “locally” evaluated from the observed signal and from the knowledge of the model (1) (see [6] for the details).

Some experimental observations of the shape parameters suggest us that the GG assumption for the distributions of the wavelet coefficients can be simplified. As to the pdf's of the wavelet coefficients of the speckle-free signal, i.e.,  $p(W_f)$ , an example of the histogram of the estimated shape parameters, obtained from the test image *Lena* degraded with 4-look synthetic speckle, is shown in Figure 1-(a): as can be seen, we may assume that they roughly approach the value 1. An analogous example, relative to the pdf's of the wavelet coefficients of the signal-dependent noise, i.e.,  $p(W_g | W_f) = p_{W_v}(W_g - W_f)$ , is shown in Figure 1-(b): in this case, we may assume that the shape parameters approach the value 2. A similar behavior has been also encountered for different subbands and different decomposition levels.

In the remainder of this paper, we will show that if we assume that the wavelet coefficients related to the speckle-free signal and to the signal-dependent noise are distributed as a Laplacian and as a Gaussian function, respectively (*LG* assumption), then the solution of the MAP equation can be found in a closed form and, therefore, with a limited computational burden.

## III. LG DESPECKLING FILTERS

### A. LG-MAP despeckling

The proposed method is based on equation (4) that, by using a simplified notation and the model in (2), can be rewritten as

$$\hat{\theta} = \arg \max_{\theta} [\log p_v(x - \theta) + \log p_{\theta}(\theta)], \quad (7)$$

where  $\theta = W_f[n]$ ,  $x = W_g[n]$ , and  $v = W_v[n]$ .

According to the experimental results mentioned in Section II-C, we will assume that the distribution of  $\theta$  is a Laplacian and that of  $v$  is a Gaussian function; specifically, they are distributed as follows:

$$p_{\theta}(\theta) = \frac{1}{\sqrt{2}\sigma_{\theta}} e^{-\frac{\sqrt{2}|\theta - \mu_{\theta}|}{\sigma_{\theta}}}, \quad p_v(v) = \frac{1}{\sqrt{2\pi}\sigma_v} e^{-\frac{(v - \mu_v)^2}{2\sigma_v^2}} \quad (8)$$

In [5], it has been demonstrated that, for the noise component  $v$ , we have

$$\mu_v = E[v] = 0, \quad (9)$$

$$\sigma_v^2 = E[v^2] = \frac{\sigma_{u'}^2}{1 + \sigma_{u'}^2} \sum_i h^2[i] E[g^2[n-i]], \quad (10)$$

where  $h[n]$  is the “equivalent” filter [5] that yields the wavelet coefficients of a given subband and  $\sigma_{u'}^2$  is the variance of the variable  $u' = u - 1$ . For the signal component  $\theta$ , instead, we have

$$\mu_\theta = E[\theta] = E[x], \quad (11)$$

$$\sigma_\theta^2 = \sigma_x^2 - E[v^2]. \quad (12)$$

From the above expressions, we can conclude that the moments of the variables  $v$  and  $\theta$  can be written as a function of the moments of the observed signal and of the observed wavelet coefficients (these quantities are estimated as local averages).

The MAP equation can be written as

$$\begin{aligned} \hat{\theta} &= \arg \max_{\theta} \left[ \log \frac{1}{\sqrt{2\pi}\sigma_v} e^{-\frac{(x-\theta)^2}{2\sigma_v^2}} + \log \frac{1}{\sqrt{2\pi}\sigma_\theta} e^{-\frac{\sqrt{2}|\theta-\mu_\theta|}{\sigma_\theta}} \right] \\ &= \arg \min_{\theta} \left[ \frac{(x-\theta)^2}{2\sigma_v^2} + \frac{\sqrt{2}|\theta-\mu_\theta|}{\sigma_\theta} \right]. \end{aligned} \quad (13)$$

The solution to this optimization problem is given by [8]

$$\hat{\theta} = \begin{cases} x - \frac{\sqrt{2}\sigma_v^2}{\sigma_\theta} & \text{if } x > \mu_\theta + \frac{\sqrt{2}\sigma_v^2}{\sigma_\theta} \\ x + \frac{\sqrt{2}\sigma_v^2}{\sigma_\theta} & \text{if } x < \mu_\theta - \frac{\sqrt{2}\sigma_v^2}{\sigma_\theta} \\ \mu_\theta & \text{elsewhere.} \end{cases} \quad (14)$$

### B. LG-MAP with Segmentation

In [7], it was demonstrated that the performance of the GG-MAP filter can be noticeably improved using a segmented approach, where each wavelet subband is divided into different classes of heterogeneity according to the texture energy of the wavelet coefficients of noise-free reflectivity. The key point is to assume that the wavelet coefficients within a particular class follow the same GG distribution, so that the parameters of the GG model can be accurately estimated within each class.

A similar approach can be applied in the case of the LG-MAP filter. Here, the key observation is that the LG model may be well suited only for a particular class of heterogeneity, whereas for other classes it may be better to use alternative models. According to the class each wavelet coefficient belongs to, we propose to apply the following three processing strategies.

- Wavelet coefficients belonging to the lower energy class are processed by means of the LG-MAP filter we propose in this paper. This class represents the set of coefficients of weakly textured areas, or homogeneous areas, which are better modeled by the assumption of Laplacian distribution.
- Wavelet coefficients belonging to the middle energy class are processed by means of the LMMSE filter proposed in [5]. The LMMSE filter is a general-purpose first-order approximation filter and it represents the optimal MAP filter when both the coefficients of noise-free reflectivity and the coefficients of speckle noise follow a normal

TABLE I  
PSNR OBTAINED BY USING *Lena* DEGRADED BY SYNTHETICALLY GENERATED SPECKLE.

	1-look	2-look	4-look	16-look
LMMSE	24.59	26.62	28.57	32.61
GG-MAP-S	26.40	28.04	29.77	33.24
LG-MAP	26.21	27.77	29.41	32.95
LG-MAP-S	26.21	27.82	29.55	33.27

TABLE II  
ORDER OF MAGNITUDE OF THE COMPUTATIONAL TIMES (IN SECONDS) OF THE ANALYZED ALGORITHMS FOR  $512 \times 512$  IMAGES. TESTS HAVE BEEN PERFORMED ON A 2.40 GHZ CPU WITH 4GB RAM.

	computational cost (s)
LMMSE	$10^1$
GG-MAP-S	$10^2$
LG-MAP	$10^1$
LG-MAP-S	$10^1$

distribution. We assume that this hypothesis is sufficiently valid for coefficients belonging to heterogeneous areas.

- Wavelet coefficients belonging to the last class are supposed to represent strongly heterogeneous areas or point targets. Because these areas do not follow any longer the fully-developed speckle model, the wavelet coefficients of the last class are left unchanged.

In the following, the above filtering strategy will be referred to as LG-MAP-S filter.

## IV. EXPERIMENTAL RESULTS

In this section, the experimental results obtained with the algorithms previously described are compared in terms of speckle removal efficiency and computational burden. In order to ascertain the performance loss/gain of the LG versus the GG assumption, a first set of quantitative results obtained by using a 8 bit  $512 \times 512$  test image (*Lena*), degraded by synthetically generated speckle noise according to the model in [6], are shown. Then, some results derived from true SAR images are also presented.

In the case of synthetically generated speckle degradation, the quality of the filtered image can be measured by means of the peak SNR (PSNR), given by  $PSNR = 10 \log_{10} 255^2 / MSE$ , where  $MSE$  is the mean square error between the original and the filtered image.

A more general method to assess the effectiveness of the different filters, which can be used also when the noise-free reference image is not available, is based on the statistics of the ratio image, defined as  $\hat{u} = g/\hat{f}$ , where  $\hat{f}$  represents the estimated noise-free reflectivity. When a fully-developed speckle model can be assumed, the above image represents the filtered out speckle noise. Hence, for a good despeckling filter  $\hat{u}$  should satisfy  $E[\hat{u}] = 1$  and  $Var[\hat{u}] = 1/L$ , where  $L$  is the number of look [1]. The mean and the variance of the ratio image are estimated by using a scatter plot method similar to that proposed in [9]. The method consists of the following steps. First, a scatter plot is obtained by plotting the occurrences of each pair of local mean and standard deviation,

TABLE III  
MEAN AND VARIANCE OF EXTRACTED NOISE  $\hat{u}$ , MEASURED ON SYNTHETICALLY CORRUPTED *Lena* THROUGH SCATTER-PLOT METHOD.

	1-look		2-look		4-look		16-look	
	$\mu_{\hat{u}}$	$\sigma_{\hat{u}}^2$	$\mu_{\hat{u}}$	$\sigma_{\hat{u}}^2$	$\mu_{\hat{u}}$	$\sigma_{\hat{u}}^2$	$\mu_{\hat{u}}$	$\sigma_{\hat{u}}^2$
LMMSE	0.9278	0.6978	0.9568	0.3602	0.9752	0.1863	0.9919	0.0465
GG-MAP-S	0.9854	0.9359	0.9883	0.4755	0.9919	0.2385	0.9966	0.0597
LG-MAP	0.9787	0.8974	0.9849	0.4553	0.9892	0.2304	0.9941	0.0576
LG-MAP-S	0.9787	0.8974	0.9848	0.4553	0.9891	0.2303	0.9945	0.0573

calculated on a moving local window over the image  $\hat{u}$ . Hence, the bivariate probability density function (pdf) is estimated from the scatter plot, and the mean and standard deviation of  $\hat{u}$  are estimated as the coordinates of the maximum of the bivariate pdf. The rationale of this method is based on the assumption that each local window would give a contribution centered on such a maximum if the size of the window is sufficiently large. Thanks to using statistics computed on local windows, the above method is accurate also in the case of real SAR images, for which the assumption of fully-developed speckle is not valid everywhere and global statistics would be biased due to the presence of outliers.

The despeckling filters that are compared in the following are: 1) the LMMSE filter [5]; the GG-MAP-S filter [7]; the LG-MAP filter proposed in section III-A; the LG-MAP-S filter proposed in section III-B. All filters use a 9/7 biorthogonal wavelet with four multiresolution levels.

In Table I, the performance of the despeckling filters are compared in terms of PSNR. The order of magnitude of the computational times, expressed in seconds and related to our Matlab implementation, are shown in Table II. As can be seen, the complexity of the LG filters is the same as the LMMSE one. However, especially for multilook images, the performance of the LG-MAP-S filter is very close to that of the GG-MAP-S filter, showing that a valuable computational gain is achieved at the price of almost unaltered performances in terms of PSNR. These results are confirmed by the observation of Table III, where the mean and the variance of  $\hat{u}$ , estimated by using the scatter plot method on the test image *Lena* for the different algorithms, are shown.

As to the results on true SAR data, they have been assessed by using a 8 bit  $512 \times 512$  4-look X-HH image representing an airport in Ontario, and a 16 bit  $1024 \times 1024$  COSMO-SkyMed 1-look X-HH image representing an area in Veneto, Italy. The original “Airport” and “COSMO-SkyMed” images are shown in Figure 2. Two portions of the above images, together with the despeckled versions obtained with the LMMSE, GG-MAP-S, LG-MAP, and LG-MAP-S filters, are shown in Figure 3. In Table IV, the mean and the variance of  $\hat{u}$ , estimated on the “Airport” and “COSMO-SkyMed” images using the scatter plot method, are shown. From Table IV, we observe that the LG methods have similar performances as the GG-MAP-S method and outperform the LMMSE one. It can be also observed that the performances of the LG-MAP and of the LG-MAP-S are almost identical, highlighting that they behave in the same way in homogeneous areas. However, comparing Figures 3-(d) and 3-(e), we observe that the LG-MAP-S yields

TABLE IV  
MEAN AND VARIANCE OF EXTRACTED NOISE  $\hat{u}$ , MEASURED ON NOMINAL 4-LOOK SAR IMAGE *Airport* AND NOMINAL 1-LOOK SAR IMAGE *COSMO-SkyMed* THROUGH SCATTER-PLOT METHOD.

	Airport		COSMO-SkyMed	
	$\mu_{\hat{u}}$	$\sigma_{\hat{u}}^2$	$\mu_{\hat{u}}$	$\sigma_{\hat{u}}^2$
LMMSE	0.9298	0.1584	0.8592	0.4044
GG-MAP-S	0.9722	0.2878	0.9237	0.5916
LG-MAP	0.9606	0.2540	0.8916	0.5463
LG-MAP-S	0.9583	0.2515	0.8905	0.5348

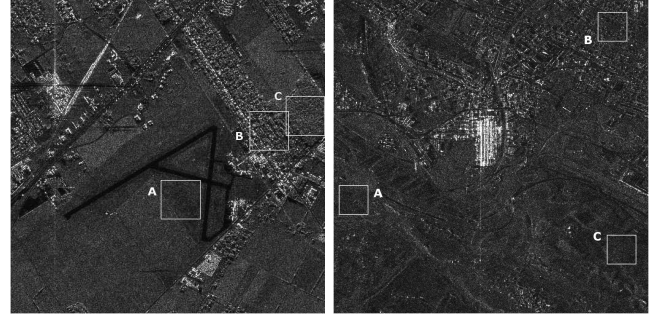


Fig. 2. SAR images “Airport” (left) and “COSMO-SkyMed” (right). The scene coefficient of variation  $C_f$  has been estimated in the highlighted areas.

a better preservation of texture details. As to the “COSMO-SkyMed” image, we notice that  $\sigma_{\hat{u}}^2$  is underestimated with respect to the nominal value 1. This is probably due to the fact that “COSMO-SkyMed” images present correlated speckle.

The effectiveness of despeckling filters on textured areas can be better evaluated by using the *scene coefficient of variation* [1], defined as  $C_f = \sqrt{(C_g^2 - \sigma_u^2)/(1 + \sigma_u^2)}$ , where  $C_g = \sigma_g/\mu_g$  is the coefficient of variation of the original image,  $\sigma_g$  and  $\mu_g$  are, respectively, the estimated standard deviation and the estimated mean of the observed signal, and  $\sigma_u$  is

TABLE V  
SCENE COEFFICIENTS OF VARIATION ( $C_f$ ) OBTAINED ON THREE  $64 \times 64$  AREAS OF *Airport* AND THREE  $96 \times 96$  AREAS OF *COSMO-SkyMed*.

	Airport			COSMO-SkyMed		
	A	B	C	A	B	C
$C_f$	0.426	1.245	0.770	0.791	3.108	0.442
LMMSE	0.367	1.002	0.606	1.048	4.118	0.502
GG-MAP-S	0.325	1.223	0.733	1.040	4.123	0.479
LG-MAP	0.312	0.937	0.530	1.016	4.100	0.437
LG-MAP-S	0.317	1.158	0.646	1.027	4.127	0.446

the estimated standard deviation of the speckle noise. Under the fully developed speckle model, an image processed by a good despeckling filter should yield a coefficient of variation  $C_{\hat{f}} = \sigma_{\hat{f}}/\mu_{\hat{f}}$  as close as possible to the corresponding  $C_f$ . The scene coefficient of variation has been evaluated on three  $64 \times 64$  areas of “Airport” and three  $96 \times 96$  areas of “COSMO-SkyMed”, characterized by different features of the underlying scene, as shown in Figure 2, and compared to the  $C_{\hat{f}}$  obtained with the different filters. The results are presented in Table V. The LG-MAP-S filter shows a behavior very close to the GG-MAP-S in each analyzed area. Interestingly, all filters tend to overestimate the  $C_f$  for the “COSMO-SkyMed” image. This is in accordance with the estimated  $\sigma_a^2$ , and can be explained by the presence of spatially correlated speckle.

## V. CONCLUSIONS

The MAP estimator, operating in the undecimated wavelet domain, with coefficients of reflectivity and noise both modeled as generalized Gaussian densities, has been demonstrated to be successful for removing speckle noise in SAR images. However, only a numerical solution, affected by a high computational burden, has been achieved. In this paper, based on the observation of the experimental histograms of the shape factors, the assumption of Laplacian reflectivity and Gaussian noise is made and a closed form solution is found. The Laplacian-Gaussian modeling is also combined with a segmentation-based approach, in which different filtering strategies are applied according to the heterogeneity of wavelet coefficients. The experimental results show that the performance of the fast algorithms, assessed on both simulated speckled images and on high-resolution SAR images, are comparable with those of the GG-based solutions, with a computational complexity more than ten times lower.

## REFERENCES

- [1] R. Touzi, “A Review of Speckle Filtering in the Context of Estimation Theory,” *IEEE Trans. on Geosci. and Remote Sens.*, vol. 40, no. 11, pp. 2392–2404, Nov. 2002.
- [2] A. Achim, P. Tsakalides, and A. Bezerianos, “SAR image denoising via Bayesian wavelet shrinkage based on heavy-tailed modeling,” *IEEE Trans. on Geosci. and Remote Sens.*, vol. 41, no. 8, pp. 1773–1784, Aug. 2003.
- [3] S. Foucher, G. B. Béné, and J.-M. Boucher, “Multiscale MAP filtering of SAR images,” *IEEE Trans. on Image Proc.*, vol. 10, no. 1, pp. 1019–1036, Jan. 2001.
- [4] S. Solbø and T. Eltoft, “Γ-WMAP: a statistical speckle filter operating in the wavelet domain,” *International Journal of Remote Sensing*, vol. 25, no. 5, pp. 1019–1036, Mar. 2004.
- [5] F. Argenti and L. Alparone, “Speckle removal from SAR images in the undecimated wavelet domain,” *IEEE Trans. on Geosci. and Remote Sens.*, vol. 40, no. 11, pp. 2363–2374, Nov. 2002.
- [6] F. Argenti, T. Bianchi, and L. Alparone, “Multiresolution MAP despeckling of SAR images based on locally adaptive generalized Gaussian pdf modeling,” *IEEE Trans. on Image Proc.*, vol. 15, no. 11, pp. 3385–3399, Nov. 2006.
- [7] T. Bianchi, F. Argenti, and L. Alparone, “Segmentation-based MAP despeckling of SAR images in the undecimated wavelet domain,” *IEEE Trans. on Geosci. and Remote Sens.*, vol. 46, no. 9, pp. 2728–2742, Sep. 2008.
- [8] H. Rabbani, M. Vafadust, P. Abolmaesumi, and S. Gazor, “Speckle noise reduction of medical ultrasound images in complex wavelet domain using mixture priors,” *IEEE Trans. on Biomedical Engineering*, vol. 55, no. 9, pp. 2152–2160, Sept. 2008.
- [9] B. Aiazzi, L. Alparone, S. Baronti, and A. Garzelli, “Coherence estimation from incoherent multilook SAR imagery,” *IEEE Trans. Geosci. Remote Sensing*, vol. 41, no. 11, pp. 2531–2539, Nov. 2003.

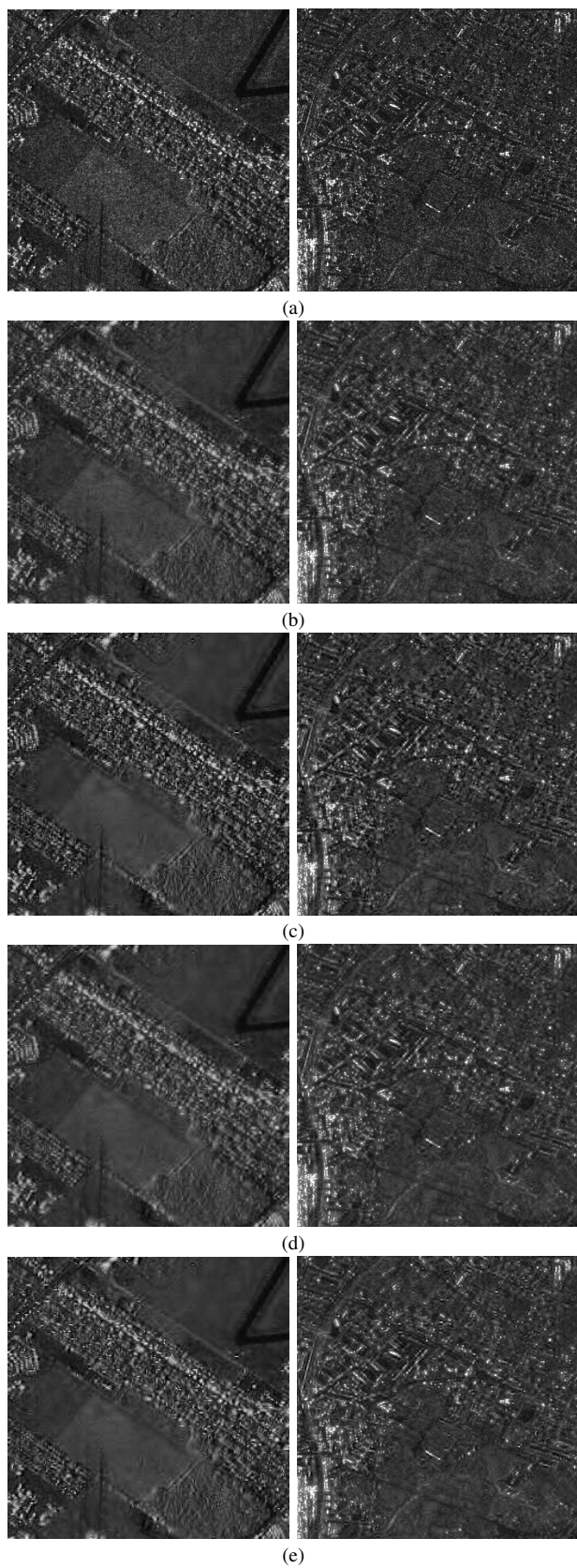


Fig. 3. Results obtained by filtering 4-look *Airport* image (left) and 1-look *COSMO-SkyMed* image (right): (a) original SAR images; (b) LMMSE; (c) GG-MAP-S; (d) LG-MAP; (e) LG-MAP-S.